that the convergence of structure in savanna conceals substantial differences in the relationships between savanna woody vegetation, climate, and fire. Just as the regional evolutionary and environmental histories underpin differences in these relationships, these same differences will determine the contemporary vegetation response of each region to future climates.

References and Notes

1. R. J. Scholes, S. R. Archer, *Annu. Rev. Ecol. Syst.* **28**, 517–544 (1997).
2. C. B. Field, M. J. Behrenfeld, J. T. Randerson, P. Falkowski, *Science* **281**, 237–240 (1998).
3. S. Archibald, C. E. R. Lehmann, J. L. Gómez-Dans, R. A. Bradstock, *Proc. Natl. Acad. Sci. U.S.A.* **110**, 6442–6447 (2013).
4. W. J. Bond, G. F. Midgley, *Glob. Change Biol.* **6**, 865–869 (2000).
5. S. I. Higgins, S. Scheiter, *Nature* **488**, 209–212 (2012).
6. I. C. Prentice, S. P. Harrison, P. J. Bartlein, *New Phytol.* **189**, 988–998 (2011).
7. J. Ratnam *et al.*, *Glob. Ecol. Biogeogr.* **20**, 653–660 (2011).
8. M. Sankaran *et al.*, *Nature* **438**, 846–849 (2005).
9. B. P. Murphy, C. E. R. Lehmann, J. Russell-Smith, M. J. Lawes, *J. Biogeogr.* **41**, 133–144 (2014).
10. W. J. Bond, *Annu. Rev. Ecol. Evol. Syst.* **39**, 641–659 (2008).
11. A. K. Knapp *et al.*, *Front. Ecol. Environ* **2**, 483–491 (2004).
12. S. Sitch *et al.*, *Glob. Change Biol.* **9**, 161–185 (2003).
13. R. Fisher *et al.*, *New Phytol.* **187**, 666–681 (2010).
14. C. E. R. Lehmann, S. A. Archibald, W. A. Hoffmann, W. J. Bond, *New Phytol.* **191**, 197–209 (2011).
15. A. C. Staver, S. Archibald, S. A. Levin, *Science* **334**, 230–232 (2011).
16. J. H. Lawton, *Oikos* **84**, 177 (1999).
17. Materials and methods and other information are available in the supplementary materials on *Science* Online.
18. S. I. Higgins, W. J. Bond, W. S. W. Trollope, *J. Ecol.* **88**, 213–229 (2000).
19. W. A. Hoffmann *et al.*, *Ecol. Lett.* **15**, 759–768 (2012).
20. B. Ripley, G. Donald, C. P. Osborne, T. Abraham, T. Martin, *J. Ecol.* **98**, 1196–1203 (2010).
21. M. Haridasan, in *Nature and Dynamics of Forest-Savanna Boundaries,* P. A. Furley, J. Proctor, J. A. Ratter, Eds. (Chapman & Hall, London, 1992), pp. 171–184.
22. E. J. Edwards *et al.*, *Science* **328**, 587–591 (2010).
23. D. M. J. S. Bowman, L. Prior, *Aust. J. Bot.* **53**, 379 (2005).
24. M. F. Simon *et al.*, *Proc. Natl. Acad. Sci. U.S.A.* **106**, 20359–20364 (2009).
25. B. J. Wigley, W. J. Bond, M. T. Hoffman, *Glob. Change Biol.* **16**, 964–976 (2010).
26. G. B. Bonan, *Science* **320**, 1444–1449 (2008).

Acknowledgments: C.L. conceived the project and led the writing; C.L., T.M.A., M.S., S.I.H., W.A.H., N.H., J.F., G.D., and S.A. compiled the data; and C.L., T.M.A., M.S., and S.I.H. analyzed the data. All authors provided new data and contributed to the writing and/or intellectual development of the manuscript. M. Crisp, B. Medlyn, and R. Gallagher provided manuscript feedback. Data used in this study are available in the supplementary materials and at http://modis.gsfc.nasa.gov/, http://www.worldclim.org/, and www.fao.org/nr/land/soils/harmonized-world-soil-database/en/.

Supplementary Materials

www.sciencemag.org/content/343/6170/548/suppl/DC1
Materials and Methods
Figs. S1 to S4
Tables S1 to S5
References (*27*–*188*)
Data Sets S1 and S2

18 October 2013; accepted 18 December 2013
10.1126/science.1247355

Effector Specialization in a Lineage of the Irish Potato Famine Pathogen

Suomeng Dong,[1] Remco Stam,[1]* Liliana M. Cano,[1] Jing Song,[2]† Jan Sklenar,[1] Kentaro Yoshida,[1] Tolga O. Bozkurt,[1] Ricardo Oliva,[1]‡ Zhenyu Liu,[2] Miaoying Tian,[2]§ Joe Win,[1] Mark J. Banfield,[3] Alexandra M. E. Jones,[1]|| Renier A. L. van der Hoorn,[4,5] Sophien Kamoun[1]¶

Accelerated gene evolution is a hallmark of pathogen adaptation following a host jump. Here, we describe the biochemical basis of adaptation and specialization of a plant pathogen effector after its colonization of a new host. Orthologous protease inhibitor effectors from the Irish potato famine pathogen, *Phytophthora infestans*, and its sister species, *Phytophthora mirabilis*, which is responsible for infection of *Mirabilis jalapa*, are adapted to protease targets unique to their respective host plants. Amino acid polymorphisms in both the inhibitors and their target proteases underpin this biochemical specialization. Our results link effector specialization to diversification and speciation of this plant pathogen.

The potato blight pathogen, *Phytophthora infestans*, is a recurring threat to world agriculture and food security. This funguslike oomycete traces its origins to Toluca Valley, Mexico, where it naturally infects wild *Solanum* plants (*1*). In central Mexico, *P. infestans* cooccurs with closely related species in a tight phylogenetic clade known as clade 1c. These species evolved through host jumps followed by adaptive specialization on plants belonging to different botanical families (*2*, *3*) (fig. S1). One species, *Phytophthora mirabilis*, is a pathogen of four-o'clock (*Mirabilis jalapa*). It split from *P. infestans* about 1300 years ago (*1*), and the two species have since specialized on their *Solanum* and *Mirabilis* hosts. Adaptive evolution after the host jump has left marks on the genomes of *P. infestans* and *P. mirabilis* (*3*). Comparative genomics analyses revealed signatures of accelerated evolution, structural polymorphisms, and positive selection in genes occurring in repeat-rich genome compartments (*3*). In total, 345 genes induced within plants show signatures of positive selection between the two sister species (*3*). These include 82 disease effector genes, rapidly evolving determinants of virulence that act on host target molecules. We lack a molecular framework to explain how plant pathogen effectors adapt and specialize on new hosts, even though this process affects pathogen evolution and diversification (*4*–*6*).

To gain insight into the molecular patterns of host adaptation after host jumps, we selected the cystatinlike protease inhibitor EPIC1, an effector protein of *P. infestans* that targets extracellular (apoplastic) defense proteases of the *Solanum* hosts (*7*, *8*). The *epiC1* gene and its paralogs *epiC2A* and *epiC2B* evolved relatively recently in the *P. infestans* lineage, most likely as a duplication of the conserved *Phytophthora* gene *epiC3* (*7*) (Fig. 1). To reconstruct the evolution of these effectors in the clade 1c species, we aligned the *epiC* gene cluster sequences, performed phylogenetic analyses, and calculated variation in selective pressure across the phylogeny (Fig. 1, fig. S2, and table S1) (*9*). We detected a signature of positive selection in the branch of *PmepiC1*, the *P. mirabilis* ortholog of *P. infestans epiC1* [nonsynonymous to synonymous ratio (ω) = 2.52] (Fig. 1B). This is consistent with our hypothesis that PmEPIC1 evolved to adapt to a *M. jalapa* protease after *P. mirabilis* diverged from *P. infestans*.

To test our hypothesis, we first determined the inhibition spectra of the EPIC effectors using DCG-04 protease profiling, a method based on the use of a biotinylated, irreversible protease inhibitor that reacts with the active site cysteine of papainlike proteases in an activity-dependent

[1]The Sainsbury Laboratory, Norwich Research Park, Norwich NR4 7UH, UK. [2]Department of Plant Pathology, Ohio Agricultural Research and Development Center, The Ohio State University, Wooster, OH 44691, USA. [3]Department of Biological Chemistry, John Innes Centre, Norwich Research Park, Norwich NR4 7UH, UK. [4]The Plant Chemetics Laboratory, Department of Plant Sciences, University of Oxford, Oxford OX1 3RB, UK. [5]Plant Chemetics Laboratory, Max Planck Institute for Plant Breeding Research, 50829 Cologne, Germany.

*Present address: Division of Plant Sciences, University of Dundee, Invergowrie, Dundee DD2 5DA, UK.
†Present address: Center for Proteomics and Bioinformatics, School of Medicine, Case Western Reserve University, Cleveland, OH 44106 USA.
‡Present address: Plant Breeding, Genetics, and Biotechnology, International Rice Research Institute (IRRI), Los Baños, Laguna, Philippines.
§Present address: Department of Plant and Environmental Protection Sciences, University of Hawaii, Honolulu, HI 96822, USA.
||Present address: School of Life Sciences, Gibbet Hill Campus, The University of Warwick, Coventry, CV4 7AL, UK.
¶Corresponding author. E-mail: sophien.kamoun@tsl.ac.uk

manner (*7*, *10*). We assayed effector activities against the tomato (*Solanum lycopersicum*) papainlike cysteine proteases RCR3, PIP1, and C14, which have been previously implicated in pathogen defense (*7*, *8*, *11*, *12*). RCR3 was inhibited by effectors EPIC1, PipEPIC1, and EPIC2B but not by PmEPIC1 (fig. S3). C14 was inhibited by all four effector proteins. PIP1 was inhibited by EPIC2B but not by the three EPIC1 effectors (fig. S3). The reduced activity of PmEPIC1 on RCR3 is not due to instability, given that this protein remained as stable as EPIC1 after a 2-hour incubation in plant apoplastic extracts (fig. S4).

P. infestans originates from central Mexico, where it naturally infects the wild potato species *Solanum demissum*, *S. verrucosum*, and *S. stoloniferum* (*2*). To challenge our model with ecologically relevant host proteases, we assayed five RCR3 homologs from these three wild potato species for their interactions with pathogen effectors EPIC1 and PmEPIC1 (fig. S5). For all three species, EPIC1 was a better inhibitor of the potato RCR3 proteases than PmEPIC1 (fig. S6). This confirms that the two orthologous effectors have evolved different biochemical activities on *Solanum* RCR3 proteases.

To identify the target of PmEPIC1 in *M. jalapa*, the natural Mexican host of *P. mirabilis*, we coincubated *M. jalapa* intercellular fluids with the EPIC1 proteins and analyzed the interactions by coimmunoprecipitation and tandem mass spectrometry (fig. S7). We compared the peptides detected with an expressed sequence tag database generated from *P. mirabilis*–infected leaves of *M. jalapa* (tables S2 and S3 and fig. S7). We consistently detected peptides matching two RCR3-related cysteine proteases. We termed the two proteases *Mirabilis* RCR3-like protease 1 and 2 (MRP1 and MRP2). We recovered the full-length proteases and found that they share ~60% amino acid sequence similarity with *Solanum* RCR3 and carry common signatures of the papainlike cysteine protease SAG12 subfamily (*13*) (fig. S8).

We transiently expressed MRP1 and MRP2 proteins as a fusion to the histidine (His) epitope tag in *M. jalapa* leaves. However, only MRP2-His can be expressed and enriched (fig. S9A). Activity profiling of the MRP2-His protein revealed that it can be labeled with the cysteine protease probe DCG-04 (*10*), and this labeling can be blocked by preincubation with the irreversible cysteine protease inhibitor E-64, which indicates that MRP2 is an active cysteine protease (fig. S9B).

To independently confirm the interaction, we performed coimmunoprecipitation experiments on enriched MRP2-His incubated with FLAG epitope–tagged EPIC proteins (*9*). Both PmEPIC1 and EPIC1 coimmunoprecipitated with MRP2-His, and the interaction could be outcompeted by E-64, which suggests that the cystatinlike effectors most likely bind to the active site of the protease (fig. S10). We then determined the extent to which the EPIC proteins inhibit MRP2-His using the DCG-04 activity profiling assay. This revealed that PmEPIC1 is more effective than EPIC1 at inhibiting MRP2-His, results counter to the activity of these effectors on *Solanum* RCR3 proteases (Fig. 2A). To further investigate these findings, we conducted a time-course DCG-04 labeling experiment. Here too, the effectors showed differential inhibition activities on MRP2-His and *S. demissum* RCR3^{dms3}-His (Fig. 2B). PmEPIC1 reduced DCG-04 labeling of MRP2-His for up to 60 min but had no noticeable effect on RCR3^{dms3}. EPIC1, in contrast, had opposite effects on DCG-04 labeling of the two proteases, as it showed stronger inhibition of RCR3^{dms3}-His than MRP2-His. These findings reveal an adaptive biochemical phenotype, with the effectors displaying increased inhibition of protease targets from their respective host plants.

We resurrected (*14*) the ancestral EPIC1 gene to test the hypothesis that the activity spectrum of EPIC1 has shifted over time. We inferred the sequence for ancestral EPIC1 using the maximum likelihood method, synthesized the corresponding gene, and determined the inhibition spectrum of the resurrected protein (fig. S11) (*9*). Ancestral EPIC1 displayed activities similar to those of modern EPIC1, i.e., stronger inhibition of RCR3^{dms3} than MRP2 (fig. S11). This indicates that the ability of PmEPIC1 to inhibit MRP2 and its inability to inhibit *Solanum* RCR3s were not characteristic of the ancestral protein.

To determine which of the variant amino acids underpin the alterations in specificity, we first took advantage of the crystal structure of tarocystatin in complex with a papain protease (Protein Data Bank ID: 3MIA) (fig. S12A). Structure-based sequence alignments of PmEPIC1 or EPIC1 with tarocystatin suggest that the inhibitors share a similar fold and are likely to bind proteases through three regions, two of which are

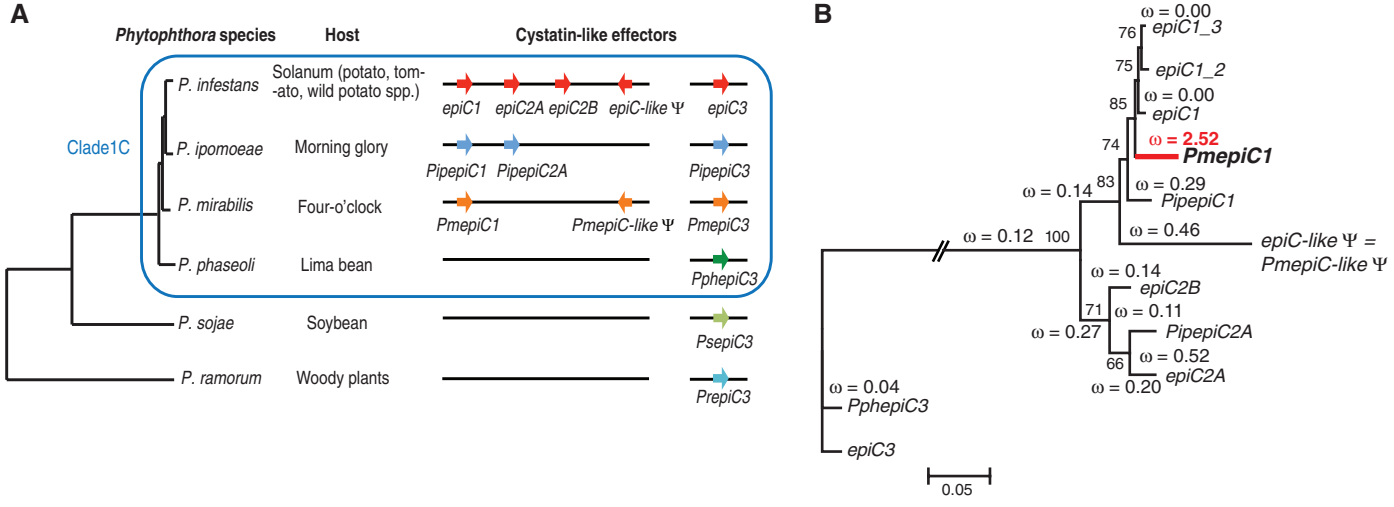

Fig. 1. Evolution of the *epiC1* gene family in *Phytophthora* clade 1c sister species. (**A**) Phylogeny, host range, and the presence or absence of polymorphisms of the *epiC1* gene family of *Phytophthora* clade 1c sister species. The *Phytophthora* phylogenetic tree was adapted from a previous publication (*15*). The positions of *P. mirabilis* and *P. ipomoeae* as closest to *P. infestans* remain to be resolved. *P. sojae* and *P. ramorum* are species from remote clades that are shown for comparison and as outgroups. The presence or absence of *epiC* genes in clade 1c is a simplified diagram of fig. S2. Arrows with colors indicate the presence of the *epiC1* homolog in genomes. The polymorphism in *Phytophthora* clade 1c and other *Phytophthora* species is consistent with the recent emergence of *epiC1* and *2* from duplication of the widespread *epiC3* gene (*7*). (**B**) Selection analysis of the *epiC1* family genes in *Phytophthora* clade 1c. The phylogenetic tree was rooted with conserved *P. infestans* gene *epiC3* using PhyML software (*9*). Rates of nonsynonymous to synonymous ratio (ω) across branches were investigated with the branch model using the codeml function provided by PAML software (*9*). Note that the PmEPIC1 branch is the only one with a strong signature of positive selection (ω = 2.52). ψ indicates a pseudogene that has lost its ability to produce the full-length protein.

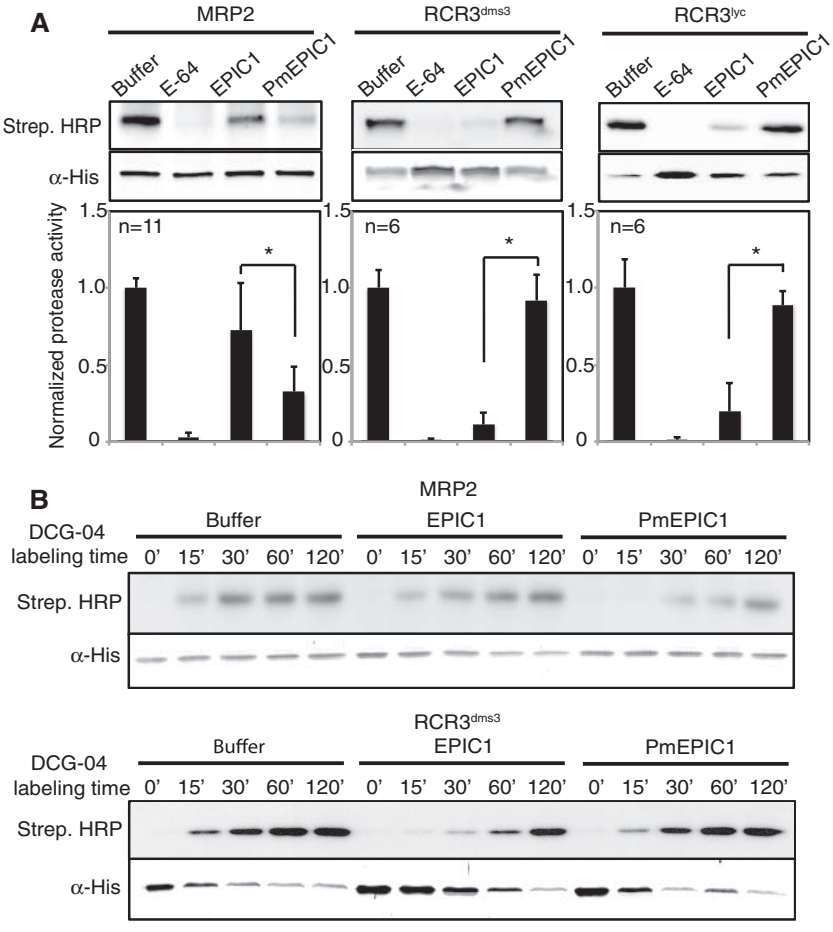

Fig. 2. The effectors EPIC1 and PmEPIC1 are stronger inhibitors of proteases from their host plants. (**A**) Inhibition activity of EPIC1 and PmEPIC1 toward *Solanum* RCR3 and *M. jalapa* MRP2 proteases. Activity profiling assays in the presence or absence of effectors revealed that FLAG-EPIC1, but not FLAG-PmEPIC1, inhibits $RCR3^{lyc}$ and $RCR3^{dms3}$-His and that FLAG-PmEPIC1 exhibits stronger inhibition of MRP2-His than FLAG-EPIC1 does. Equal amounts of *Nicotiana benthamiana* apoplastic fluid containing $RCR3^{lyc}$-His and $RCR3^{dms3}$-His or MRP2-His enriched from *M. jalapa* apoplastic fluids were preincubated with excess E-64 (200 μM) or recombinant EPIC1 or PmEPIC1 (4 μM) for 1 hour, followed by DCG-04 (100 nM) labeling for 30 min (*9*). Biotinylated proteases were detected by streptavidin–horseradish peroxidase (Strep. HRP). α-His, antibody against histidine. Protease activities were quantified, normalized, and presented as means ± SEM. *$P < 0.05$ (Wilcoxon rank-sum test). (**B**) Time-course inhibition assay confirms inhibition specificity of EPIC1 and PmEPIC1. Apoplastic fluids containing $RCR3^{dms3}$-His and enriched MRP2-His proteins were preincubated with an excess of FLAG-EPIC1 and FLAG-PmEPIC1 (4 μM) for 1 hour, followed by addition of DCG-04 (200 nM) to label the proteases. Reactions were stopped at different time points to record inhibition of protease activity over time.

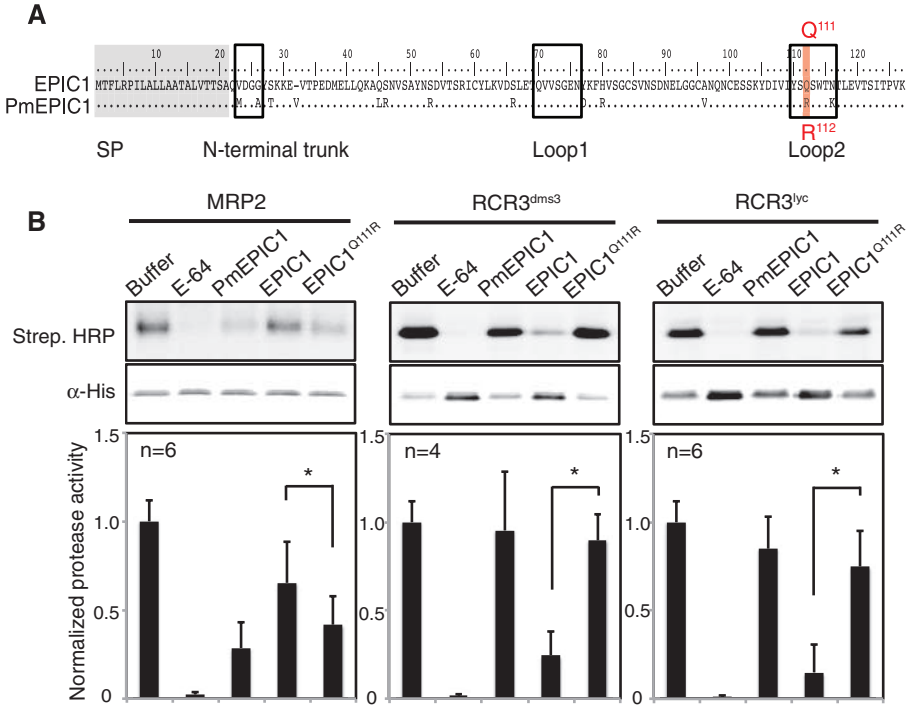

Fig. 3. $EPIC1^{Q111R}$ mutant can inhibit MRP2 but is impaired in RCR3 inhibition. (**A**) Amino acid sequence alignment of EPIC1 and PmEPIC1 highlighting the key residue 111. Residues predicted to bind to cysteine proteases are highlighted in boxes. Gln^{111}/Arg^{112} is in red. Predicted signal peptides are in gray. (**B**) Inhibition of $EPIC1^{Q111R}$ toward $RCR3^{lyc}$, $RCR3^{dms3}$, and MRP2. Activity profiling assays in the presence or absence of effectors were performed as described in the methods (*9*). Protease activities were quantified and normalized. Data are presented as means ± SEM. *$P < 0.05$ (Wilcoxon rank-sum test).

polymorphic between the orthologous effectors (fig. S12). Next, we modified the proteins to determine which of the polymorphic residues contribute to the difference in biochemical activity. Protease inhibition assays with chimeric proteins and with single-site mutants revealed that the Gln-Arg polymorphism at position 111 is critical for specificity (Fig. 3 and figs. S13 and S14). In particular, EPIC1^{Q111R}, carrying a Gln-to-Arg mutation, most closely recapitulated the function of PmEPIC1, with more effective inhibition of the *M. jalapa* protease MRP2 and less inhibition of the *Solanum* proteases RCR3^{dmx3} and RCR3^{lyc} (*S. lycopersicum*) (Fig. 3). Sequences of *epiC1* or *PmepiC1* alleles from 26 *P. infestans* isolates and 9 *P. mirabilis* isolates indicated that the key Gln or Arg residue is fixed in each population (table S1 and fig. S11).

We also investigated which variant amino acids determine specificity in the proteases. Inspection of the tarocystatin-papain complex identified a protease region that interacts with a tarocystatin residue equivalent to the EPIC1 or PmEPIC1 key Gln or Arg residue (fig. S15A). Structure-based sequence alignments of RCR3 or MRP2 with papain indicated that the inhibitor-binding region overlaps with a seven–amino acid region that is polymorphic between RCR3 and MRP2 (fig. S15, B and C). We constructed proteases altered in this region by swapping the entire seven–amino acid domain or by single–amino acid changes. The results revealed the polymorphic residue His^{148} or Asn^{147} in RCR3 and Asp^{152} in MRP2 as a key element of specificity (figs. S16 and S17). Unlike wild-type RCR3 proteases, RCR3^{H148D} and RCR3^{N147D} mutants with a single His to Asp or Asn to Asp mutation could be inhibited by PmEPIC1 (fig. S17). This suggests that effector PmEPIC1 adaptation to host protease MRP2 was in part driven by the occurrence of Asp^{152} in the *M. jalapa* protease.

Thus, in this case of oomycete infection of potato and four o'clock flower, a single–amino acid polymorphism in the host protease and a reciprocal single–amino acid change in the pathogen effectors underpin the ecological diversification (fig. S18). The arginine substitution found in the *P. mirabilis* effector may enhance effector inhibition of the *M. jalapa* protease. This same substitution would impair interaction with Asn^{147} of RCR3^{dmx3} and His^{148} of RCR3^{lyc} and so provide a molecular explanation for how this effector works on one protease but not the other (fig. S19).

References and Notes

1. K. Yoshida *et al.*, *eLife* **2**, e00731 (2013).
2. N. J. Grünwald, W. G. Flier, *Annu. Rev. Phytopathol.* **43**, 171–190 (2005).
3. S. Raffaele *et al.*, *Science* **330**, 1540–1543 (2010).
4. B. A. Roy, *Evolution* **55**, 41–53 (2001).
5. S. Raffaele, S. Kamoun, *Nat. Rev. Microbiol.* **10**, 417–430 (2012).
6. E. H. Stukenbrock, *New Phytol.* **199**, 895–907 (2013).
7. M. Tian *et al.*, *Plant Physiol.* **143**, 364–377 (2007).
8. J. Song *et al.*, *Proc. Natl. Acad. Sci. U.S.A.* **106**, 1654–1659 (2009).
9. Materials and methods are available as supplementary material on *Science* Online.
10. R. A. L. van der Hoorn, M. A. Leeuwenburgh, M. Bogyo, M. H. Joosten, S. C. Peck, *Plant Physiol.* **135**, 1170–1178 (2004).
11. F. Kaschani *et al.*, *Plant Physiol.* **154**, 1794–1804 (2010).
12. M. Shabab *et al.*, *Plant Cell* **20**, 1169–1183 (2008).
13. K. H. Richau *et al.*, *Plant Physiol.* **158**, 1583–1599 (2012).
14. J. W. Thornton, *Nat. Rev. Genet.* **5**, 366–375 (2004).
15. J. E. Blair, M. D. Coffey, S. Y. Park, D. M. Geiser, S. Kang, *Fungal Genet. Biol.* **45**, 266–277 (2008).

Acknowledgments: We thank D. G. O. Saunders for comments on drafts of the manuscript and C. Taylor, M. D. Coffey, and V. Vleeshouwers for providing biomaterial. This project was funded by the Gatsby Charitable Foundation, the U.K. Biotechnology and Biological Sciences Research Council, the Ohio Agricultural Research and Development Center at The Ohio State University, and a National Research Initiative of the U.S. Department of Agriculture grant OHO00963–SS. Sequences are deposited in GenBank under the submission accession numbers provided in (*9*).

Supplementary Materials

www.sciencemag.org/content/343/6170/552/suppl/DC1
Materials and Methods
Supplementary Text
Figs. S1 to S19
Tables S1 to S5
References (*16*–*36*)

23 September 2013; accepted 11 December 2013
10.1126/science.1246300